

## Characterisation of the influence of vanadium and tantalum on yttrium-based nano-oxides in ODS Eurofer steel

Fu, J.; Davis, T. P.; Kumar, A.; Richardson, I. M.; Hermans, M. J.M.

**DOI**

[10.1016/j.matchar.2021.111072](https://doi.org/10.1016/j.matchar.2021.111072)

**Publication date**

2021

**Document Version**

Final published version

**Published in**

Materials Characterization

**Citation (APA)**

Fu, J., Davis, T. P., Kumar, A., Richardson, I. M., & Hermans, M. J. M. (2021). Characterisation of the influence of vanadium and tantalum on yttrium-based nano-oxides in ODS Eurofer steel. *Materials Characterization*, 175, Article 111072. <https://doi.org/10.1016/j.matchar.2021.111072>

**Important note**

To cite this publication, please use the final published version (if applicable).  
Please check the document version above.

**Copyright**

Other than for strictly personal use, it is not permitted to download, forward or distribute the text or part of it, without the consent of the author(s) and/or copyright holder(s), unless the work is under an open content license such as Creative Commons.

**Takedown policy**

Please contact us and provide details if you believe this document breaches copyrights.  
We will remove access to the work immediately and investigate your claim.



# Characterisation of the influence of vanadium and tantalum on yttrium-based nano-oxides in ODS Eurofer steel

J. Fu<sup>a,b,\*</sup>, T.P. Davis<sup>c</sup>, A. Kumar<sup>a</sup>, I.M. Richardson<sup>a</sup>, M.J.M. Hermans<sup>a</sup>

<sup>a</sup> Department of Materials Science and Engineering, Delft University of Technology, Delft, the Netherlands

<sup>b</sup> Dutch Institute for Fundamental Energy Research (DIFFER), Eindhoven, the Netherlands

<sup>c</sup> Department of Materials, University of Oxford, Parks Road, Oxford OX1 3PH, United Kingdom

## ARTICLE INFO

### Keywords:

Oxide dispersion strengthened steel  
ODS Eurofer  
Atom probe tomography  
Microstructure  
Nanoclusters

## ABSTRACT

Oxide dispersion strengthened (ODS) steels are leading candidates for structural materials in nuclear fission and fusion power plants. Understanding the nature of nano-oxide particles in ODS steels is vital for a better control of the microstructure and mechanical properties to further their applications. In this study, electron microscopy and atom probe tomography (APT) have been used to investigate the nanocluster features in ODS Eurofer steel. With the addition of V and Ta in ODS Eurofer, the nanoclusters exhibit a higher number density with a decreased average diameter, indicating that V and Ta are beneficial for the formation of small clusters. Irrespective of the composition of the base material, the smaller particles have a variable stoichiometry while the larger particles are likely to have Y<sub>2</sub>O<sub>3</sub> stoichiometry. The nanoclusters were found to have a core/shell structure, where Y, O and Ta are enriched in the core and Cr and V are predominant in the shell. The formation of the complex structure is possibly the result of a competing effect between Ta, Y, V and Cr binding with O. It is deduced that Ta tends to combine with O in the core (Y<sub>2</sub>O<sub>3</sub>) of the clusters due to a higher affinity, and pushes V and Cr to the surrounding shell during the formation of nanoclusters.

## 1. Introduction

Reduced activation ferritic/martensitic (RAFM) steels are candidate materials for structural applications in high temperature and nuclear applications including advanced fission and fusion reactors [1]. However, the operating temperature of RAFM steels is limited to around 823 K due to their poor creep resistance. By the small addition (0–0.5 wt%) of nanosized yttrium oxide (Y<sub>2</sub>O<sub>3</sub>) in the steel matrix, the operating temperature of these RAFM steels can be increased by 100–200 K due to a significant increase in the creep and fatigue properties [2–4]. These fine and thermally stable dispersoids hinder the motion of dislocations and pin grain boundaries, and act as effective trapping sites for both point defects and helium atoms generated during irradiation [5]. Currently, oxide dispersion strengthened (ODS) steels are under intense development in Europe [6], Japan [7], South Korea [8] and the US [9] and are considered as promising structural materials for nuclear applications. Within the European Union, the research of ODS steels has essentially been focused on ODS Eurofer, which is based on Eurofer 97 steel and reinforced with 0.3 wt% Y<sub>2</sub>O<sub>3</sub> [10]. Compared to RAFM steels,

ODS Eurofer possesses better high temperature mechanical properties, improved creep resistance and significantly higher irradiation damage resistance.

Considering the important role that the oxide particles play in affecting the performance of ODS Eurofer, it is crucial that their characteristics, such as size distribution, chemical composition, morphology and number density, are well understood. Previous investigations on the oxide particles in ODS steels were conducted by means of different techniques, the results, however, were not completely consistent with each other. For example, Williams et al. [11] found a core/shell structure in ODS Eurofer via atom probe tomography (APT), where the core is primarily composed of Y and O enriched with Mn and Si, while C, N, Ta, W, V and Cr were predominantly found in the shell. Klimenkov et al. [12] reported transmission electron microscopy (TEM) investigations of ODS Eurofer steel, suggesting that the nanoparticles were more than 10 nm with a complex structure. The core of the particle consisted of a phase with a composition of (Y<sub>1.8</sub>Mn<sub>0.2</sub>)O<sub>3</sub>, which was surrounded by a shell of V and Cr with 0.5–1.5 nm thickness. Such a complex composition of the ODS particles led to the assumption that their nucleation and

\* Corresponding author at: Department of Materials Science and Engineering, Delft University of Technology, Delft, the Netherlands.

E-mail addresses: [j.fu@tudelft.nl](mailto:j.fu@tudelft.nl) (J. Fu), [thomas.davis@davisusgrove.com](mailto:thomas.davis@davisusgrove.com) (T.P. Davis), [ankit.kumar@asml.com](mailto:ankit.kumar@asml.com) (A. Kumar), [I.M.Richardson@tudelft.nl](mailto:I.M.Richardson@tudelft.nl) (I.M. Richardson), [M.J.M.Hermans@tudelft.nl](mailto:M.J.M.Hermans@tudelft.nl) (M.J.M. Hermans).

<https://doi.org/10.1016/j.matchar.2021.111072>

Received 26 January 2021; Received in revised form 25 March 2021; Accepted 26 March 2021

Available online 29 March 2021

1044-5803/© 2021 The Author(s). Published by Elsevier Inc. This is an open access article under the CC BY license (<http://creativecommons.org/licenses/by/4.0/>).

dispersion was associated with the concentrations of Mn and Y. An APT study on ODS Eurofer from Aleev et al. [13] revealed that the core of nanoclusters was rich in V, Y and O while the concentration of Mn was negligible in the clusters. A model Fe–12Cr–0.4Y<sub>2</sub>O<sub>3</sub> (wt%) alloy was investigated by Castro et al. [14] using electron energy loss spectroscopy (EELS), after annealing at 1023 K up to 96 h, the nanoparticles either had a core/shell structure with a Cr-enriched shell or evolved into complex oxides such as YCrO<sub>3</sub>. Furthermore, studies on Ti containing ODS steels gave even more complex findings. Ohnuma et al. [15] used small angle scattering using neutrons (SANS) and X-rays (SAXS) to study a number of 9Cr–ODS steels containing Ti and found that the finest oxide nanoparticles have a chemical composition close to Y<sub>2</sub>Ti<sub>2</sub>O<sub>7</sub>. Recent APT analysis of a Fe–18Cr–1W–0.3Ti–0.3Y<sub>2</sub>O<sub>3</sub> (wt%) ODS steel [16] showed that the Y–O–Ti nanoparticles exhibited a core–shell structure consisting of a complex Cr-rich shell with 1.2–1.5 nm thickness. The particle stoichiometry evolved from YTiO<sub>2</sub> for the small particles (<2 nm) to Y<sub>2</sub>TiO<sub>5</sub> for the big ones (>8 nm). Templeman et al. [17] used a combined investigation method of TEM, APT and electron diffraction tomography (EDT) to characterise a Fe–14Cr–1W–0.3Ti–0.25 Y<sub>2</sub>O<sub>3</sub> (wt%) ODS steel. Three populations of particles were identified: highly dispersed, 3–20 nm Fe(Cr,Ti,Y)O particles, 50–150 nm YTiO<sub>3</sub> and 100–200 nm TiC particles. In summary, there have been considerable uncertainties in terms of characterising and understanding the nature of nanoclusters in ODS Eurofer/ODS steels. Part of the inconsistency undoubtedly comes from the differences in alloy compositions, processing routes employed, and techniques and interpretation methods used for the characterisation of nanoclusters in ODS steels. A thorough understanding of the nano-oxide characteristics is needed for a better control of microstructure and mechanical properties for ODS steels and their nuclear applications.

In this study, the nanoclusters in ODS Eurofer were characterised and investigated by means of scanning electron microscopy (SEM), TEM and APT. The composition and structure of nanoclusters were determined by a careful interpretation of APT datasets. The results of ODS Eurofer and ODS Eurofer with extra V and Ta are compared and discussed to understand the effect of alloying elements on the nature of nanoclusters. Providing insights into possible mechanisms of nanocluster formation, this paper will contribute to the optimisation of ODS steels with a desired microstructure and superior mechanical performance for nuclear applications.

## 2. Experimental details

### 2.1. Materials

ODS Eurofer steel with a nominal composition of Fe–9Cr–1.1W–0.4Mn–0.2V–0.12Ta–0.1C–0.3Y<sub>2</sub>O<sub>3</sub> (wt%) was manufactured using high-purity elemental powders. The mixed powders were mechanically alloyed (MA) in a Retsch planetary mill for 30 h with a rotation speed of 300 rpm under a high-purity argon atmosphere at room temperature. The MA powders were then consolidated by spark plasma sintering (SPS, FCT group, Germany) to form a dense cylindrical pellet (40 mm in diameter and 10 mm in height). Sintering cycles were performed under a pressure of 60 MPa, with a heating rate of 100 K/min up to the holding temperature of 1373 K for 30 min. The cooling was ensured by direct contact with water-cooled punches, which induced a cooling rate of 50 K/min. These parameters were selected based on our previous study [18]. To characterise the effect of V and Ta on the nano-precipitates more accurately, ODS Eurofer with extra V and Ta and a nominal composition of Fe–9Cr–1.1W–0.4Mn–2V–1.2Ta–0.1C–0.3Y<sub>2</sub>O<sub>3</sub> (wt%) was manufactured with the same parameters stated above. The material is referred to as “ODS Eurofer–2V–1.2Ta” in the following text.

### 2.2. Microscopy analysis

The microstructure of ODS Eurofer was initially investigated using a

JEOL 6500F scanning electron microscope (SEM) and a JEM-2200FS transmission electron microscope (TEM) equipped with an energy dispersive spectrometer (EDS) system. For TEM characterisation, conventional thin foils were extracted from the investigated steel samples. Small disks, 3 mm in diameter were cut and ground down to a thickness of around 80 μm. The thickness of TEM specimens was further reduced by electropolishing in a twin-jet electropolisher using 4% perchloric acid and 96% ethanol as electrolyte at room temperature.

Atom probe analyses of ODS Eurofer and ODS Eurofer–2V–1.2Ta were conducted with a CAMECA LEAP® 5000XR at the Department of Materials, University of Oxford. Atom probe specimens were prepared by the lift-out technique [19] using a Zeiss Crossbeam 540 Analytical Focused Ion Beam (FIB)-SEM. Cleaning of the specimens was performed using 2 kV Ga ions to minimise FIB-induced damage. The atom probe tips were cooled down to 55 K. A 355 nm wavelength, frequency tripled Nd:YAG laser at 40 pJ and 200 kHz was used to sputter atoms from the tip under ultra-high vacuum, at an average detection rate of 1.0%. The detection efficiency of the LEAP 5000XR is 52% [20]. CAMECA IVAS® 3.8.4 software was used to reconstruct the 3D chemical atomic maps. SEM micrographs of the final tip shape and crystallographic pole indexing were used for reconstruction of the APT maps. A maximum separation method was used to study the nanoclusters [21] with the following parameters:  $N_{\min} = 10$ , order = 1,  $d_{\max}$  ranging from 0.8–1.5 nm and  $L = d_{\text{erosion}} = 0.5d_{\max}$ . The size, number density and composition of nano-clusters were calculated using the solute ions of VN, YO, Y, O and TaO<sub>2</sub>.

## 3. Results and discussion

### 3.1. SEM and TEM observations

Fig. 1 shows an SEM image of the microstructure of ODS Eurofer. The material has an average grain size of around 2 μm. A large number of precipitates (50–200 nm) was found to be present preferably along the grain boundaries in the material. EDS analysis indicated that the precipitates were rich in Fe, Cr, W and C, which can be identified as M<sub>23</sub>C<sub>6</sub> carbides (M = Fe, Cr and W) based on their size and chemical composition. The presence of M<sub>23</sub>C<sub>6</sub> carbides is commonly found in chromium containing steels (Davis et al. [22] observed these carbides in APT). They can play an important role in affecting the mechanical properties of the material such as strength, toughness and ductility depending on their size and morphology [23]. In addition, a high number density of nano-precipitates can be observed in the steel matrix. Fig. 2 shows a TEM micrograph of an enlarged area of the ODS Eurofer steel. Two distinct particle size distributions can be seen within the microstructure:

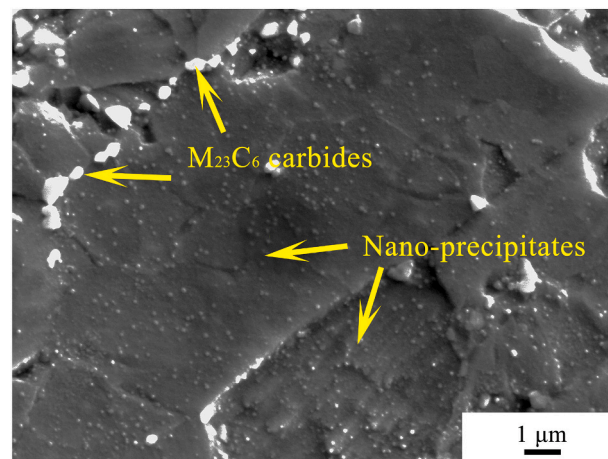
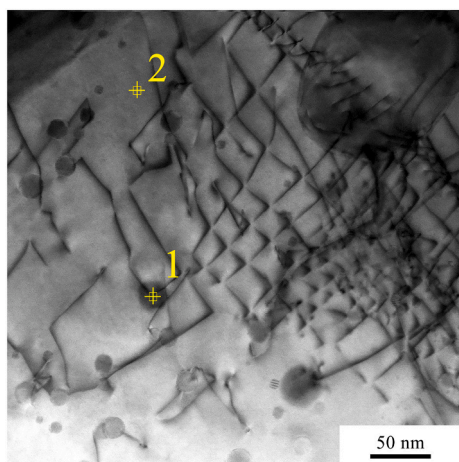


Fig. 1. An SEM micrograph of ODS Eurofer showing M<sub>23</sub>C<sub>6</sub> carbides and nano-precipitates.



**Fig. 2.** A TEM image of ODS Eurofer showing large and small nano-precipitates interacting with dislocations.

large (5–15 nm) and small (1–5 nm). The pinning effect by these nanoparticles on the dislocations is clearly manifested in the micrograph, which could lead to an enhanced creep resistance compared to non-ODS steels. The chemical composition of a large precipitate (#1, Fig. 2) was measured by STEM–EDS and is shown in Table 1. It can be seen that the precipitate is a Y-O based nanoparticle enriched in alloying elements. The V and Ta contents are significantly higher in the particle compared to the matrix, indicating a segregation effect and preferential solute element clustering. The Y/O atom ratio is around 0.56. Due to the resolution limitation of the TEM equipment used [24], EDS was unable to resolve and characterise the composition of nano-precipitates smaller than 3 nm.

### 3.2. APT analysis

In order to accurately characterise the finely dispersed nano-oxide particles in ODS Eurofer, APT was conducted to perform cluster analysis on the atomic scale. Table 2 summarises the concentrations of elements in ODS Eurofer averaged over 5 analysed tips irrespective of their spatial distribution. The matrix composition was estimated from data that excluded the atoms of clusters in the volumes. In general, there is a good agreement between the X-ray fluorescence (XRF, for heavy elements) and LECO analysis (for C) measured chemical composition and the APT measured results, indicating that the identifications of ion species within the APT mass-spectrum is reasonable. The measured C content is lower than the chemical composition. Due to the low solubility of C in bcc Fe, it can be assumed that the majority of C is likely to have segregated and formed carbides (such as  $M_{23}C_6$ ) and is not captured in the APT datasets due to the small volume probed. The matrix composition is depleted with Y and O, probably due to the formation and segregation of the Y-O clusters. More importantly, according to Ref. [11,

**Table 1**

Chemical composition of a nano-precipitate and the matrix of ODS Eurofer shown in Fig. 2.

Element (wt%)	#1	#2
C	0.51	0.06
Si	–	0.07
Cr	10.28	9.06
Fe	51.78	88.78
W	0.87	0.75
V	9.48	0.34
Y	15.04	0.11
O	4.83	0.36
Mn	0.90	0.55
Ta	6.28	0.02

[13] on the structure of nanoclusters in ODS steels, V and Ta can play an important role in affecting the formation of nano-oxides. Due to the low level of V and Ta detected by APT, ODS Eurofer–2V–1.2Ta were made and analysed to further investigate their influences on the nature of nanoclusters. The chemical and APT measured compositions of the modified material are also presented in Table 2.

Three dimensional elemental maps of ODS Eurofer and ODS Eurofer–2V–1.2Ta were obtained by APT and are shown in Fig. 3. In ODS Eurofer (Fig. 3(a)), elements of Fe, Cr, Mn, W, C and Si were relatively homogeneously distributed in the analysed volume. The elemental distribution of Fe is shown as an example with a uniform distribution. Elemental maps of V, O, and Y show non-homogenous distribution (i.e. clustering) features, indicating an enrichment of these solute elements in the nanoclusters. In addition, molecular ions of VO, YO and TaO<sub>2</sub> have been identified from the mass spectrum and overlap with previously mentioned clusters, providing confidence that they contribute towards the cluster analysis. In the case of ODS Eurofer–2V–1.2Ta (Fig. 3(b)), the ion point cloud maps quantitatively reveal a higher density of nanoclusters in the sample. The averaged number density of the clusters is  $5.15 \times 10^{23} \text{ m}^{-3}$  compared to  $2.44 \times 10^{23} \text{ m}^{-3}$  found in ODS Eurofer. Moreover, it is notable that the size and spatial distributions of the nanoclusters are not homogenous in either condition (a common feature in ODS steels [25]). The corresponding size distribution of nanoclusters is shown in Fig. 4. The size of nanoclusters varies from 1.8–12.2 nm, with the average value of 4.13 nm in ODS Eurofer, while that in ODS Eurofer–2V–1.2Ta ranges from 1.2–14 nm, with the average value of 2.96 nm. The experimental results suggest that the addition of V and Ta appears to affect and promote the formation of small, high density nanoclusters.

The averaged chemical composition of the nanoclusters in ODS Eurofer is shown in Table 3. The measured Fe by APT is around 36.56 at. %, which is probably the result of trajectory aberrations [11]. Although it is possible that nano-oxides contain Fe, it is very unlikely that such a high level of Fe is present in the core of the particles, due to a very low solubility of Fe in Y<sub>2</sub>O<sub>3</sub> [26]. The exact quantity of Fe in the clusters is not addressed in this study. Instead, following the method proposed by Williams et al. [11], the Fe contribution in the clusters was artificially set to zero. The Fe level was used to estimate the quantity of the other matrix elements introduced by trajectory aberrations, which were removed from the raw composition. The obtained cluster composition is quoted as “matrix corrected” in Table 3. It can be seen that the clusters in ODS Eurofer are mainly composed of V, Y and O and enriched with other alloying elements. The averaged chemical composition of the nanoclusters in ODS Eurofer–2V–1.2Ta were measured and corrected by the same method. Of noted interest, the Ta level is significantly higher, while the V level is lower compared to the clusters in ODS Eurofer. This could be due to the addition of Ta in the material. Considering that Ta has a higher affinity for O than V [27], it is possible that Ta combines with O in Y<sub>2</sub>O<sub>3</sub> and pushes V to the outside of the particle core.

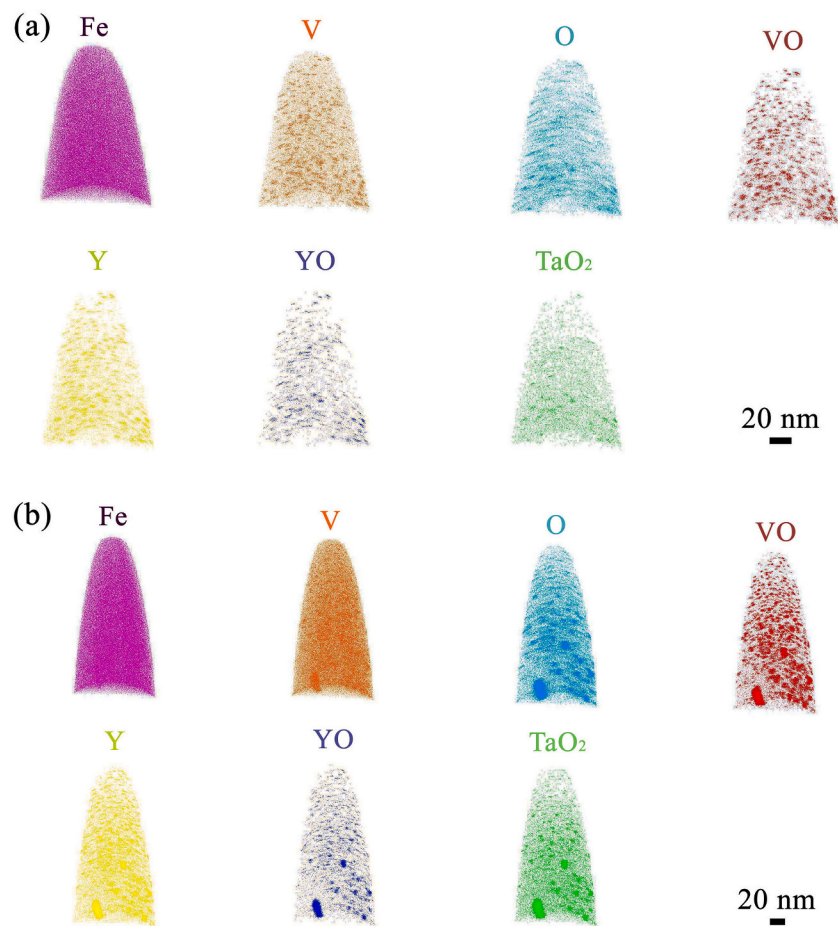
To further investigate the composition difference in small and large clusters, the averaged chemical composition of clusters larger than 6 nm in ODS Eurofer and clusters larger than 4 nm in ODS Eurofer–2V–1.2Ta were measured and are shown in Table 3. It can be seen that in both cases, the Ta and Cr level increase and the Y level slightly decreases for the large clusters. This indicates that there are more Ta and Cr atoms contributing to the formation of large nanoclusters, leading to a lower level of Y in the clusters.

The Y/O ratio of nanoclusters in ODS Eurofer and ODS Eurofer–2V–1.2Ta are plotted in Fig. 5. In both cases, the smaller clusters have a variable stoichiometry, while in the larger clusters, the Y/O ratio shows a relatively constant value of around  $0.51 \pm 0.16$ , which is in good agreement with the TEM analysis. (It is worth mentioning that, while no crystallographic measurements were conducted to determine the stoichiometry, the compositional measurements indicate what the stoichiometry would be.) In addition, the Y/O ratio of the larger clusters in ODS Eurofer–2V–1.2Ta is slightly lower than that in ODS Eurofer,

**Table 2**

X-ray fluorescence and LECO analysis measured and APT measured compositions of ODS Eurofer and ODS Eurofer-2V-1.2Ta.

Element	ODS Eurofer by XRF/LECO (at.%)	ODS Eurofer bulk by APT (at.%)	ODS Eurofer matrix by APT (at.%)	ODS Eurofer-2V-1.2Ta by XRF/LECO (at.%)	ODS Eurofer-2V-1.2Ta bulk by APT (at.%)	ODS Eurofer-2V-1.2Ta matrix by APT (at.%)
C	0.42	0.02	0.08	0.43	0.05	0.11
Si	0.02	0.04	0.05	0.02	0.04	0.05
Cr	9.16	9.03	9.14	9.52	9.01	9.17
Fe	89.05	89.99	90.11	86.47	88.56	88.94
W	0.28	0.30	0.25	0.31	0.24	0.30
N	–	0.04	0.02	–	0.07	0.03
V	0.19	0.18	0.13	2.1	1.06	0.98
Y	0.12	0.06	0.02	0.13	0.14	0.05
O	0.21	0.20	0.06	0.22	0.60	0.19
Mn	0.53	0.13	0.16	0.45	0.14	0.14
Ta	0.03	0.01	0.01	0.33	0.08	0.03

**Fig. 3.** APT 3D reconstruction of (a) ODS Eurofer and (b) ODS Eurofer-2V-1.2Ta.

probably due to a higher number of molecular ions of VO and TaO<sub>2</sub> in the clusters.

Two one-dimensional concentration profiles obtained from a cylinder of 2 nm diameter and intercepting an interested particle are shown in Fig. 6. One particle of around 2.5 nm diameter in ODS Eurofer (Fig. 6 (a)) and one particle of around 8 nm diameter in ODS Eurofer-2V-1.2Ta (Fig. 6(b)) were analysed. By examining the cross-sectional composition profiles, it appears that the particles have a pronounced core/shell structure. It can be seen that Cr and V have higher levels near the particle-matrix interface, forming the shell, whereas Y, O and Ta are more concentrated at the core. The level of other alloying elements (excluding Fe) in the shell and core of the particles is lower than 0.5 at.% and does not seem to play an important role in affecting the structure of nanoclusters. The formation of the core/shell structure in our study is

possibly due to a segregation of elements to the particle/matrix interface. As Ta and Y have a higher affinity for O than Cr and V, Ta and Y tend to bind with O in the particle core, while some of the Cr and V are pushed to the surrounding shell. Another possible reason proposed by Williams et al. [11] is that the shell can act as an interfacial phase in nanoparticles, lowering the surface energy and promoting the formation of nanoparticles.

The composition of ODS steels should be carefully designed to fulfil the requirements for the cladding structure in nuclear power plants. For example, the addition of Cr was to achieve a better corrosion resistance while W was used to replace Mo, Nb, and Ni in conventional ferritic steels to obtain low activation capability [28]. In this study, the important role of V and Ta in cluster formation is confirmed by an analysis of the mass spectrum of the evaporated particles. It has been

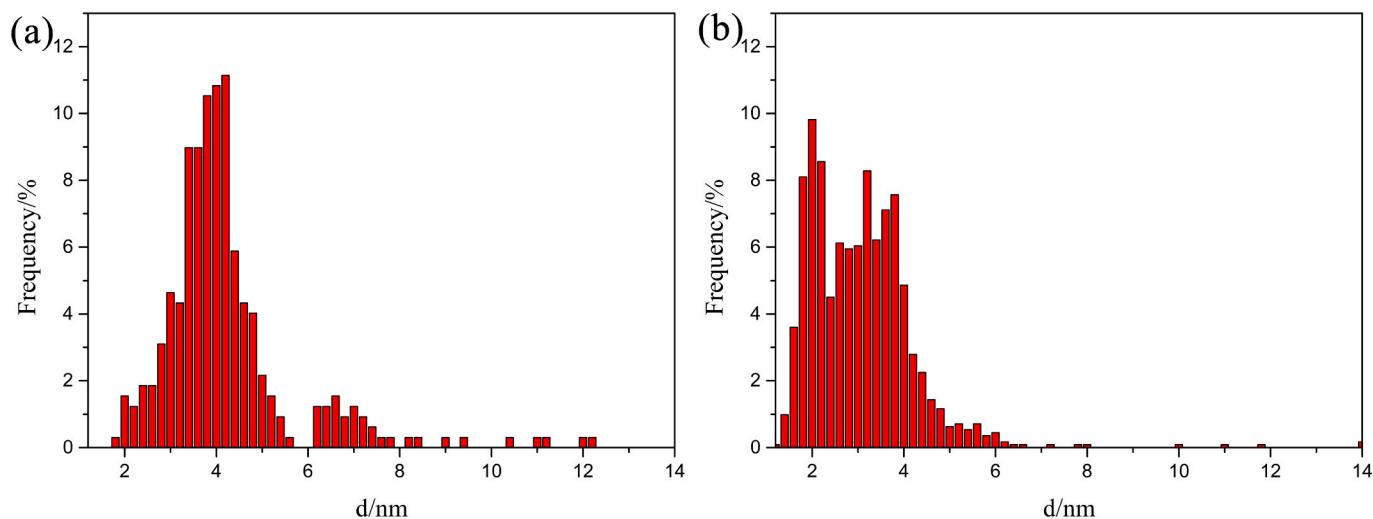


Fig. 4. Size distribution of nanoclusters in (a) ODS Eurofer and (b) ODS Eurofer-2V-1.2Ta.

Table 3

Averaged chemical composition of the nanoclusters in ODS Eurofer and ODS Eurofer-2V-1.2Ta.

Element	Nanoclusters in ODS Eurofer		Clusters larger than 6 nm in ODS Eurofer		Nanoclusters in ODS Eurofer-2V-1.2Ta		Clusters larger than 4 nm in ODS Eurofer-2V-1.2Ta	
	Measured (at. %)	Matrix corrected (at.%)	Measured (at. %)	Matrix corrected (at.%)	Measured (at. %)	Matrix corrected (at.%)	Measured (at. %)	Matrix corrected (at.%)
C	0.04	0.02	0.08	0.09	0.05	0.03	0.09	0.07
Si	0.08	0.10	0.16	0.30	0.04	0.04	0.10	0.13
Cr	6.19	4.18	8.97	8.76	2.96	1.19	5.25	2.83
Fe	36.56	0.00	50.4	0.00	19.70	0.00	33.93	0.00
W	0.13	0.05	0.21	0.16	0.09	0.03	0.19	0.12
N	4.18	6.95	2.87	6.49	7.77	9.97	4.99	8.05
V	16.72	28.13	11.21	25.29	15.42	19.53	13.23	20.79
Y	13.27	22.22	9.02	20.45	19.72	25.32	12.67	20.45
O	22.60	37.99	16.62	37.66	29.26	37.53	25.03	40.35
Mn	0.08	0.13	0.13	0.09	0.05	0.03	0.14	0.15
Ta	0.15	0.24	0.32	0.72	4.94	6.34	4.38	7.06

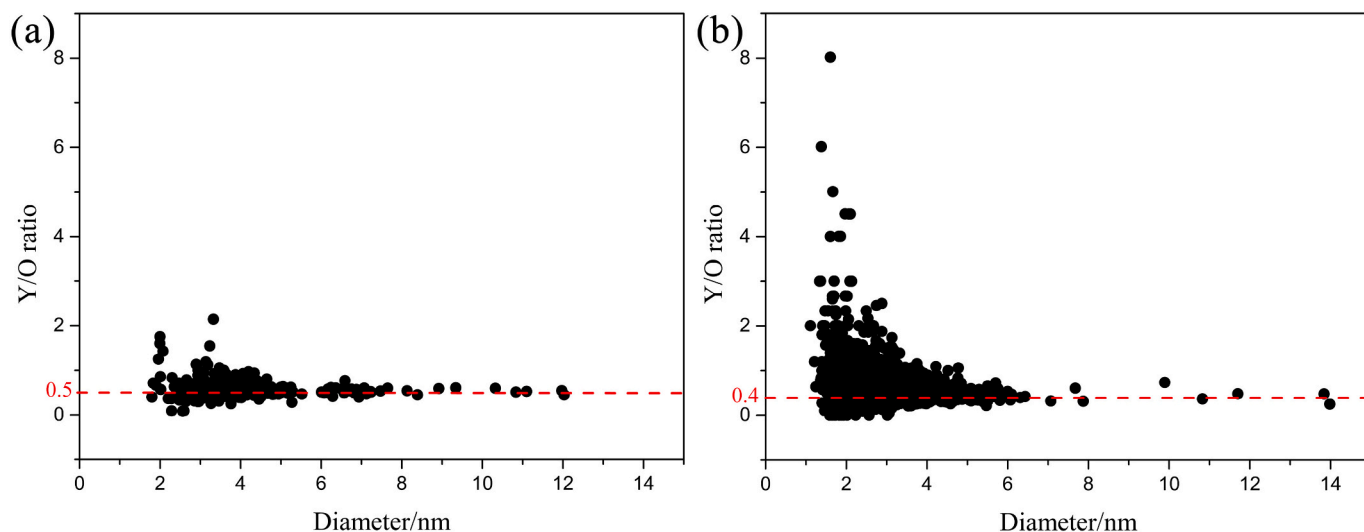


Fig. 5. Y/O ratio of nanoclusters in (a) ODS Eurofer and (b) ODS Eurofer-2V-1.2Ta.

revealed that, apart from ions and isotopes such as  $\text{Cr}^{+2}$ ,  $\text{V}^{+2}$ ,  $\text{Y}^{+3}$ , and  $\text{O}^{+}$ , a number of molecular ions, such as  $\text{CrO}_2^{+3}$ ,  $\text{YO}^{+2}$ ,  $\text{VO}^{+2}$ ,  $\text{VO}_2^{+1}$ ,  $\text{TaO}_2^{+1}$  and  $\text{TaO}_2^{+2}$ , were identified from the mass spectrum. It should be noted that the evaporation of such ions is possible only if there is a large

affinity between the atoms [29]. It is likely that there is a competition effect between Cr, Y, V and Ta binding with O when forming nanoclusters, suggesting how and why Cr, V and Ta solute elements enter the core of  $\text{Y}_2\text{O}_3$  particles. However, whether the formation of  $\text{Y}_2\text{O}_3$  particles

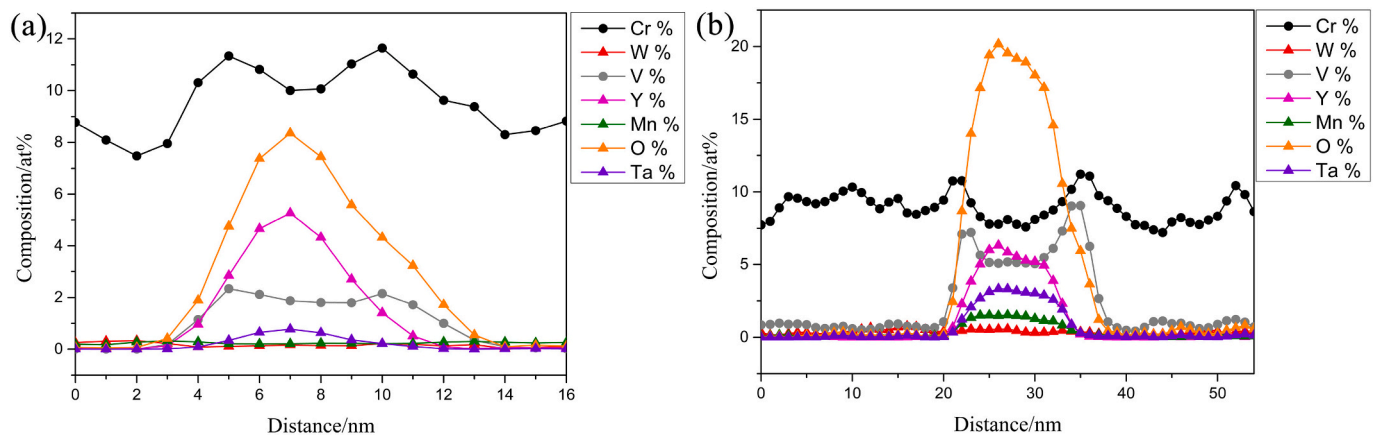


Fig. 6. Composition profiles along the direction of analysis, intercepting a representative particle in (a) ODS Eurofer and (b) ODS Eurofer-2V-1.2Ta.

occurs before or after the oxidation of vanadium and tantalum is beyond the scope of this study. Considering the high level of V and Ta in the nanoclusters irrespective of size and composition, at least it cannot be excluded that V and Ta can act as nucleation sites for  $Y_2O_3$  clusters.

By subtracting the O atoms in molecular ions composed of Cr, V, Ta and O, the calculated Y/O ratios at the core of the small and large particle in Fig. 6 are around 1.58 and 0.69, respectively. According to Williams et al. [11] and Miller et al. [30], oxygen atoms in the clusters in ODS steels generally have a greater radius of gyration than the segregated metal atoms. This could cause a slightly underestimated oxygen level when using the maximum separation method to define clusters. Therefore, the core of the larger particle is likely to have  $Y_2O_3$  stoichiometry, assuming that the actual Y/O ratio is close to 0.67. This finding is consistent with the results found by Sakasegawa et al. [31] and He et al. [32], which concluded that the composition of nanoclusters could be affected by their size and the larger particles tend to have a stable phase of yttrium oxide ( $Y_2O_3$ ).

#### 4. Conclusions

Nanoclusters in ODS Eurofer and ODS Eurofer-2V-1.2Ta steels were characterised by means of SEM, TEM and APT. The following conclusions from this study were as follows:

- (1) The nanoclusters have a number density of  $2.44 \times 10^{23} \text{ m}^{-3}$  with an average diameter of 4.13 nm in ODS Eurofer in comparison with a number density  $5.15 \times 10^{23} \text{ m}^{-3}$  with an average diameter of 2.96 nm in ODS Eurofer-2V-1.2Ta. The addition of V and Ta appears to influence and promote the formation of small, high density nanoparticles.
- (2) There is a difference in composition between the small particles (<4 nm) and large particles (around 5–15 nm). The small particles have a variable stoichiometry while the large particles are likely to have  $Y_2O_3$  stoichiometry.
- (3) Cross-sectional composition measurements show that the nanoparticles have a core/shell structure. Y, O and Ta are found to be enriched in the core whereas Cr and V are predominantly present in the shell, which is possibly due to a competition of elements binding with O.

APT is a powerful tool to characterise nanocluster features in ODS steels. However, the operating conditions and data interpretation need to be carefully addressed to obtain self-consistent and valid results to be compared to other characterisation techniques.

#### Data availability

The raw/processed data required to reproduce these findings cannot be shared at this time due to technical or time limitations.

#### Declaration of Competing Interest

No potential conflict of interest was reported by the authors.

#### Acknowledgements

This research was carried out under project number T16010f in the framework of the Partnership Program of the Materials innovation institute M2i ([www.m2i.nl](http://www.m2i.nl)) and the Netherlands Organisation for Scientific Research ([www.nwo.nl](http://www.nwo.nl)). The authors thank the industrial partner Nuclear Research and Consultancy Group (NRG) in this project for the financial support. T. P. Davis is funded by the Clarendon Scholarship from the University of Oxford and United Kingdom's Engineering and Physical Sciences Research Council (EPSRC) Fusion Centre for Doctorial Training [EP/L01663X/1]. APT was supported by grant EP/M022803/1 "A LEAP 5000XR for the UK National Atom Probe Facility".

#### References

- [1] M. Nagini, K. Pradeep, R. Vijay, A. Reddy, B. Murty, G. Sundararajan, A combined electron microscopy, atom probe tomography and small angle X-ray scattering study of oxide dispersion strengthened 18Cr ferritic steel, *Mater. Charact.* 110306 (2020).
- [2] K.D. Zilnyk, H.R.Z. Sandim, R.E. Bolmaro, R. Lindau, A. Möslang, A. Kostka, D. Raabe, Long-term microstructural stability of oxide-dispersion strengthened Eurofer steel annealed at 800 °C, *J. Nucl. Mater.* 448 (2014) 33–42.
- [3] I. Kuběna, J. Polák, P. Marmy, T. Kruml, A comparison of microstructure evolution due to fatigue loading in Eurofer 97 and ODS Eurofer steels, *Proc. Eng.* 74 (2014) 401–404.
- [4] G. Yu, N. Nita, N. Baluc, Thermal creep behaviour of the EUROFER 97 RAFM steel and two European ODS EUROFER 97 steels, *Fusion Eng. Des.* 75 (2005) 1037–1041.
- [5] M.K. Dash, R. Mythili, R. Ravi, T. Sakthivel, A. Dasgupta, S. Saroja, S.R. Bakshi, Microstructure and mechanical properties of oxide dispersion strengthened 18Cr-ferritic steel consolidated by spark plasma sintering, *Mater. Sci. Eng. A* 736 (2018) 137–147.
- [6] C. Eiselt, H. Schendzielorz, A. Seubert, B. Hary, Y. De Carlan, P. Diano, B. Perrin, D. Cedat, ODS-materials for high temperature applications in advanced nuclear systems, *Nucl. Mater. Energy* 9 (2016) 22–28.
- [7] S. Ukai, N. Oono-Hori, S. Ohtsuka, *Oxide Dispersion Strengthened Steels*, 2019.
- [8] T.K. Kim, S. Noh, S.H. Kang, J.J. Park, H.J. Jin, M.K. Lee, J. Jang, C.K. Rhee, Current status and future prospective of advanced radiation resistant oxide dispersion strengthened steel (ARROS) development for nuclear reactor system applications, *Nucl. Eng. Technol.* 48 (2016) 572–594.
- [9] S. Zinkle, J. Boutard, D. Hoelzer, A. Kimura, R. Lindau, G. Odette, M. Rieth, L. Tan, H. Tanigawa, Development of next generation tempered and ODS reduced activation ferritic/martensitic steels for fusion energy applications, *Nucl. Fusion* 57 (2017), 092005.

- [10] R. Mateus, P. Carvalho, D. Nunes, L. Alves, N. Franco, J.B. Correia, E. Alves, Microstructural characterization of the ODS Eurofer 97 EU-batch, *Fusion Eng. Des.* 86 (2011) 2386–2389.
- [11] C.A. Williams, E.A. Marquis, A. Cerezo, G.D. Smith, Nanoscale characterisation of ODS–Eurofer 97 steel: an atom-probe tomography study, *J. Nucl. Mater.* 400 (2010) 37–45.
- [12] M. Klimenkov, R. Lindau, A. Möslang, TEM study of internal oxidation in an ODS–Eurofer alloy, *J. Nucl. Mater.* 386 (2009) 557–560.
- [13] A. Alev, N. Iskandarov, M. Klimenkov, R. Lindau, A. Möslang, A. Nikitin, S. Rogozhkin, P. Vladimirov, A. Zaluzhnyi, Investigation of oxide particles in unirradiated ODS Eurofer by tomographic atom probe, *J. Nucl. Mater.* 409 (2011) 65–71.
- [14] V. De Castro, E. Marquis, S. Lozano-Perez, R. Pareja, M. Jenkins, Stability of nanoscale secondary phases in an oxide dispersion strengthened Fe–12Cr alloy, *Acta Mater.* 59 (2011) 3927–3936.
- [15] M. Ohnuma, J. Suzuki, S. Ohtsuka, S.-W. Kim, T. Kaito, M. Inoue, H. Kitazawa, A new method for the quantitative analysis of the scale and composition of nanosized oxide in 9Cr-ODS steel, *Acta Mater.* 57 (2009) 5571–5581.
- [16] C. Hatzoglou, B. Radiguet, P. Pareige, Experimental artefacts occurring during atom probe tomography analysis of oxide nanoparticles in metallic matrix: quantification and correction, *J. Nucl. Mater.* 492 (2017) 279–291.
- [17] Y. Templeman, S. Rogozhkin, A. Khomich, A. Nikitin, M. Pinkas, L. Meshi, Characterization of nano-sized particles in 14% Cr oxide dispersion strengthened (ODS) steel using classical and frontier microscopy methods, *Mater. Charact.* 160 (2020) 1110075.
- [18] J. Fu, J. Brouwer, I. Richardson, M. Hermans, Effect of mechanical alloying and spark plasma sintering on the microstructure and mechanical properties of ODS Eurofer, *Mater. Des.* 177 (2019) 107849.
- [19] M.K. Miller, K.F. Russell, K. Thompson, R. Alvis, D.J. Larson, R. Anderson, S. Klepeis, J. Cairney, D. Saxey, D. Mcgrouter, Review of atom probe FIB-based specimen preparation methods, *Microsc. Microanal.* 13 (2007) 428–436.
- [20] T.L. Martin, A.J. London, B. Jenkins, S.E. Hopkin, J.O. Douglas, P.D. Styman, P. A. Bagot, M.P. Moody, Comparing the consistency of atom probe tomography measurements of small-scale segregation and clustering between the LEAP 3000 and LEAP 5000 instruments, *Microsc. Microanal.* 23 (2017).
- [21] J. Hyde, C. English, Symposium R: Microstructural Processes in Irradiated Materials, *Mater. Res. Soc. Symp. Proc.*, 2000, p. R6.
- [22] T.P. Davis, J.C. Haley, S. Connolly, M.A. Auger, M.J. Gorley, P.S. Grant, P.A. Bagot, M.P. Moody, D.E. Armstrong, Electron microscopy and atom probe tomography of nanoindentation deformation in oxide dispersion strengthened steels, *Mater. Charact.* 167 (2020) 110477.
- [23] L. Zheng, X. Hu, X. Kang, D. Li, Precipitation of M23C6 and its effect on tensile properties of 0.3C-20Cr-11Mn-1Mo-0.35N steel, *Mater. Des.* 78 (2015) 42–50.
- [24] Y. Miao, K. Mo, Z. Zhou, X. Liu, K.-C. Lan, G. Zhang, M.K. Miller, K.A. Powers, Z.-G. Mei, J.-S. Park, On the microstructure and strengthening mechanism in oxide dispersion-strengthened 316 steel: a coordinated electron microscopy, atom probe tomography and in situ synchrotron tensile investigation, *Mater. Sci. Eng. A* 639 (2015) 585–596.
- [25] A. Das, P. Chekhonin, E. Altstadt, F. Bergner, C. Heintze, R. Lindau, Microstructural characterization of inhomogeneity in 9Cr ODS EUROFER steel, *J. Nucl. Mater.* 152083 (2020).
- [26] D. Murali, B. Panigrahi, M. Valsakumar, S. Chandra, C. Sundar, B. Raj, The role of minor alloying elements on the stability and dispersion of yttria nanoclusters in nanostructured ferritic alloys: an ab initio study, *J. Nucl. Mater.* 403 (2010) 113–116.
- [27] Y.-R. Luo, *Comprehensive Handbook of Chemical Bond Energies*, CRC Press, 2007.
- [28] R. Lindau, A. Möslang, M. Rieth, M. Klimiankou, E. Materna-Morris, A. Alamo, A.-A. Tavassoli, C. Cayron, A.-M. Lancha, P. Fernandez, Present development status of EUROFER and ODS-EUROFER for application in blanket concepts, *Fusion Eng. Des.* 75 (2005) 989–996.
- [29] S. Rogozhkin, A. Alev, A. Zaluzhnyi, N. Iskanderov, A. Nikitin, P. Vladimirov, R. Lindau, A. Möslang, Atom probe tomography of nanoscaled features of oxide-dispersion-strengthened ODS Eurofer steel in the initial state and after neutron irradiation, *Phys. Met. Metallogr.* 113 (2012) 98–105.
- [30] M. Miller, E. Kenik, K. Russell, L. Heatherly, D. Hoelzer, P. Maziasz, Atom probe tomography of nanoscale particles in ODS ferritic alloys, *Mater. Sci. Eng. A* 353 (2003) 140–145.
- [31] H. Sakasegawa, F. Legendre, L. Boulanger, M. Brocq, L. Chaffron, T. Cozzika, J. Malaplate, J. Henry, Y. de Carlan, Stability of non-stoichiometric clusters in the MA957 ODS ferritic alloy, *J. Nucl. Mater.* 417 (2011) 229–232.
- [32] J. He, F. Wan, K. Sridharan, T.R. Allen, A. Certain, V. Shutthanandan, Y. Wu, Stability of nanoclusters in 14YWT oxide dispersion strengthened steel under heavy ion-irradiation by atom probe tomography, *J. Nucl. Mater.* 455 (2014) 41–45.